International Journal of Pharmaceutics 414 (2011) 233–243

Contents lists available at ScienceDirect

International Journal of Pharmaceutics

journal homepage: www.elsevier.com/locate/ijpharm

Pharmaceutical Nanotechnology

A novel tumor-targeted delivery system with hydrophobized hyaluronic acid–spermine conjugates (HHSCs) for efficient receptor-mediated siRNA delivery

Yan Shen[a], Buhai Wang[b,*,1], Yang Lu[c], Ammar Ouahab[a], Qian Li[d,*], Jiasheng Tu[a,**]

[a] Department of Pharmaceutics, China Pharmaceutical University, Nanjing 210009, China
[b] Department of Oncology, Subei People's Hospital of Jiangsu Province, Yangzhou, Jiangsu 225001, China
[c] Department of Industrial Pharmacy, School of Chinese Pharmacy, Beijing University of TCM, Beijing 100102, China
[d] School of Life Science and Technology, China Pharmaceutical University, Nanjing 210009, China

ARTICLE INFO

Article history:
Received 15 January 2011
Received in revised form 15 April 2011
Accepted 18 April 2011
Available online 23 April 2011

Keywords:
Hyaluronic acid
Small interfering RNA
HA-receptor
Tumor-targeted
HA-receptor mediated endocytosis

ABSTRACT

A novel target specific small interfering RNA (siRNA) delivery system was successfully developed using hydrophobized hyaluronic acid–spermine conjugates (HHSCs), which were previously synthesized and their properties were also characterized in our published papers. Fluorescein isothiocyanate (FITC) labeled specific Silencer Select siRNAs were used as a model system suppressing the cyclooxygenase-2 (COX-2) gene expression. The polymers were able to effectively bind siRNA, self-assemble into micelles, protect siRNA from degradation by nuclease and release complexed siRNA efficiently in the presence of low concentrations of polyanionic heparin. The cytotoxicity of siRNA/HHSCs complex to SGC-7901 cells was lower than that of siRNA/PEI 25k and Lipofectamine 2000 complex according to the MTT assay. When SGC-7901 and GES-1 cells were treated with FITC labeled siRNA/HHSCs complexes, SGC-7901 cells, with a cluster determinant 44 receptor (CD_{44}), showed higher green fluorescent intensity than GES-1 cells because of the HA receptor mediated endocytosis of the complex. In addition, the inhibitory effect on the uptake in the presence of free HA in the transfection medium revealed that siRNA/HHSC-1 complex was selectively taken up to SGC-7901 cells via HA-receptor mediated endocytosis. Based on flow cytometry and microscopy, observation revealed that siRNA/HHSC complex was taken up preferentially through caveolae-mediated endocytosis, which may be a desirable pathway for avoiding the lysosomal degradation of delivered genes. All these results demonstrated that the intracellular delivery of siRNA/HHSC complex could be facilitated by the HA-receptor mediated endocytosis.

1. Introduction

RNA interference (RNAi) with small interfering RNA (siRNA) holds a great potential for the treatment of human diseases by silencing specific disease related genes (Hannon, 2002; Soutschek et al., 2004). Due to its fast degradation in the physiological milieu, poor cellular uptake, inefficient translocation into the cytoplasm, and lack of targeting ability, delivery of synthetic small interfering RNA (siRNA) remains the major obstacle to its therapeutic application. Therefore, it is essential to incorporate siRNA into a delivery system to improve siRNA stability and cellular uptake, which may also reduce non-specific RNAi activities of free siRNA (Kleinman et al., 2008). To overcome these problems, siRNA is often complexed with cationic lipids or cationic polymers to form nanoparticles through charge interactions for facilitating intracellular delivery to improve its cellular uptake, enhance stability from enzymatic attack, as well as facilitating siRNA release in the cytoplasm to silence specific genes after endocytosis (Oishi et al., 2005; Prakash et al., 2005; Schiffelers et al., 2004; Wilson et al., 2005). But cationic polymeric carriers such as polyethylenenimine (PEI) could facilitate endosomal escape of nanoparticles with high buffering capacity generally exhibit high cytotoxicity. Liposome-based carriers often require "helper lipids" such as dioleoyl phosphatidylethanolamine (DOPE) and subsequent extensive formulation optimization to achieve good transfection. Cationic polymers are required for negatively charged poly(alky acids) to form stable delivery systems with nucleic acids (Wang et al., 2009).

Recently the ability of sperminated polysaccharides (including dextrans) to give polyplexes useful for gene delivery has been tested (Eliyahu et al., 2006b). Spermine is a tetraamine involved in cellular metabolism and present in all eukaryotic cells (Azzam et al.,

* Corresponding authors.
** Corresponding author. Tel.: +86 2583271305; fax: +86 2583301606.
E-mail addresses: wbhself@sina.com (B. Wang), leqean@163.com (Q. Li), jiashengtu@cpu.edu.cn (J. Tu).
[1] These authors contributed equally to this work.

0378-5173/$ – see front matter.
doi:10.1016/j.ijpharm.2011.04.049

2004). The transfection efficiency of sperminated polysaccharides, assessed with various cell lines and gene markers was found to be depending on the content of grafted spermine. Polycations with higher spermine content resulted in high gene expression, whereas lower spermine content resulted in low transfection efficiencies (Cavallaro et al., 2008). Moreover hydrophobized sperminated polysaccharides such as dextran–spermine derivatives with fatty acids and cholesterol showed improved transfection yields in comparison to unmodified sperminated polysaccharides due to the role played in stability and uptake of polycation/DNA complexes by the hydrophobic portions (Eliyahu et al., 2006a, 2007).

Hyaluronic acid (HA) is a naturally occurring nonsulfated glycosaminoglycan (GAG) polysaccharide composed of N-acetyl-D-glucosamine and D-glucuronic acid and is a major constituent of the extracellular matrix (ECM) (Turley, 1989). Moreover, HA regulates angiogenesis in many types of tumors, and HA receptors such as CD_{44} and RHAMM are abundantly presented in tumor cells (Coradini et al., 1999; Luo et al., 2000; Yerushalmi et al., 1994). Consequently, these tumor cells show enhanced binding and internalization of HA, and it has been shown that these bioconjugates with HA are internalized into cancer cells through receptor-mediated endocytosis, followed by intracellular release of active drugs, thus restoring their original cytotoxicity (Eliaz and Szoka, 2001; Elron-Gross et al., 2008; Jiang et al., 2008, 2009; Lee et al., 2007; Surace et al., 2009; Yerushalmi and Margalit, 1998).

In our recent publications (Shen et al., 2009), hyaluronic acid grafted hydrophobic amines and spermine conjugates were synthesized, which were self-aggregated in water to form nanoparticles. Degree of substitution of spermine (DS_p, μmol/mg) was determined by 2,4,6-trinitro-benzenesulfonic acid (TNBS) assay. The amount of conjugated hydrophobic amines (DS_a, mol/mol) in HHSCs was quantitatively characterized from the ^1H NMR spectra by using the integration method. The resulting modified conjugates could form self-assembled nanoparticles with a size of 125–555 nm, which was significantly dependent on the DS_a and the chain length of the hydrophobic groups. The conjugates were able to form at highly diluted concentrations as low as 40–140 mg/L with the zeta potential about +20 mV which might provide their potential for targeted siRNA delivery.

In this study, fluorescein isothiocyanate (FITC) labeled specific Silencer Select siRNAs for cyclooxygenase-2 (COX-2), which are frequently overexpressed in gastric cancer, were used as a model system. We investigated whether hydrophobized hyaluronic acid–spermine conjugate (HHSC) demonstrates improved transfection efficiency in HA receptor (CD_{44}) over-expressing SGC-7901 cells compared to polyethylenimine with a high molecular weight of 25,000 Da (PEI 25k) and Lipofectamine®. Receptor-mediated tumor targeting behavior of siRNA/HHSC complex was evaluated in vitro by competitive inhibition with free-HA. Their cytotoxicity, stability for the efficient siRNA delivery and the mechanism of cellular uptake were also evaluated.

2. Materials and methods

2.1. Materials

Synthetic FITC-siRNA for COX-2 was obtained from GenePharma Co., Ltd. Hyaluronic acid grafted hydrophobic amines (laurylamine) and spermine conjugates, which called HHSC-1, HHSC-2 and HHSC-3 with HA molecular weight (M_W) 9600 Da (DS_p was 2.67, 3.16 and 3.34 μmol/mg, respectively, while DS_a was 27.6, 21.3 and 14.8 mol/mol, respectively) were synthesized according to our published papers (Shen et al., 2009) The synthesis route and characterizations could be found in figure captions. Lipofectamine®, branched polyethylenimine (PEI, M_W 25k), PEI (M_W 600), phenylarsine oxide (phAsO), amiloride, filipin III from *Streptomyces filipinensis*, MTT assay Kit and penicillin/streptomycin solution were purchased from Sigma–Aldrich (St. Louis, MO). Fetal bovine serum (FBS), Dulbecco's modified Eagle's medium (DMEM) and RPMI 1640 medium were purchased from Gibco BRL (Grand Island, NY). Reagents for cell culture, RNase-free distilled water, and SYBR® gold (nucleic acid gel stain) were purchased from Invitrogen (Carlsbad, CA). All other chemicals and reagents were of analytical grade.

2.2. Methods

2.2.1. Preparation and binding ability of siRNA/HHSCs complex

The siRNA/HHSC complex was prepared by mixing 1 mL of FITC labeled siRNA (100 mM) with the specified amount of HHSCs (HHSC-1, HHSC-2 and HHSC-3) solution (10 mg/mL) followed by incubation at room temperature for 15 min (Jeon et al., 2008; Jere et al., 2009). The weight ratio of HHSCs to siRNA varied from 0.5 to 10. The complex formation was confirmed by gel electrophoresis. The siRNA and siRNA/HHSCs complexes were loaded in the wells of 2.0 wt% agarose gel containing a SYBR® gold at concentration of 0.01 mg/mL, which was applied to 90 V electrodes in 50 mM borate buffer (pH 8.98) for 20 min. The siRNA was visualized by SYBR® gold staining and the gel image was taken under UV. The pictures were digitized and analyzed with Scion image analysis software to determine the mean density of siRNA bands. The binding percentage was calculated based on the relative intensity of free siRNA band in each well with respect to wells with free siRNA (i.e., in the absence of any conjugate). The binding for each conjugate was tested at least in 3 independent experiments.

2.2.2. Stability of siRNA/HHSC complex

The stability of siRNA/HHSC complexes was investigated using a heparin polyanion competition assay (Bolcato-Bellemin et al., 2007; Mok and Park, 2008) and a serum stability assay (Breunig et al., 2008; Kim et al., 2006). For the heparin polyanion competition assay, complexes were prepared at weight ratio (HHSCs:siRNA) of 5:1 to ensure complete binding of siRNA by the conjugates, and then incubated with varying concentrations of Heparin (0.25, 0.5, 1.0, 2.0, 3.0 U/μg siRNA) at 37 °C for 1 h. The solutions were run on agarose gel as described earlier. Results were presented as average of at least 3 independent experiments.

To evaluate the stability of the complexes in serum condition, siRNA/HHSC complexes were prepared at different polymer to siRNA weight ratios, ranging between 4:1 and 32:1, and incubated with 25% fetal bovine serum (FBS) for 24 h at 37 °C. At the same time, free siRNA, Lipofectamine/siRNA and PEI/siRNA (1:1 in weight ratio) were incubated with 25% FBS at 37 °C for 24 h as the negative and positive controls, respectively. Samples were then incubated for 1 h with excess of heparin (2.0 U/μg siRNA) to ensure complete release of siRNA from the formulation. The intact siRNA percentage was then analyzed by agarose gel electrophoresis as described earlier. The results shown represent an average of at least 3 independent experiments.

2.2.3. Cell lines and cell culture

We selected a human gastric adenocarcinoma and a normal gastric cell lines for this study. SGC-7901 (Shanghai Institute of Cell Research, Shanghai, China) is an adherent, moderately differentiated, human gastric adenocarcinoma cell line. The cell lines are gastric cancer epithelial cells and grow as adherent cells in RPMI 1640 (Hyclone Inc., USA) containing 10% FCS. GES-1 cells derived from a human fetal gastric mucosa epithelium (Ke et al., 1994), were purchased from Beijing Institute for Cancer Research. The cells were routinely cultured in DMEM supplemented with 100 U/mL penicillin, 100 U/mL streptomycin, and 10% fetal bovine serum (FBS), under 5% CO_2/95% air. The cultures were then incubated at 37 °C,

with 5% CO_2 and saturated humidity; culture transfer was performed once every 2–3 days.

2.2.4. MTT assay

The cytotoxicity was evaluated by the MTT assay. SGC-7901 cells were aliquoted into a 96-well plate (4×10^3 cells/well) and incubated at 37 °C for 24 h. The prepared siRNA/HHSCs complex, siRNA/PEI complex and siRNA/Lipofectamine complex (a weight ratio from 1:1 to 1:200) solutions (20 μL each) were incubated at room temperature for 20 min and added to the cells in the absence of FBS. HA solution (M_w: 9600) without siRNA was used as a control. At the end of the transfection step, 20 μL of 2 mg/mL MTT solution in PBS was added to the plate and incubated at 37 °C for additional 4 h. The medium containing MTT was removed and 300 μL of DMSO was added to dissolve the formazan crystal formed by live cells. The optical density was measured at 540 nm with UV spectrophotometer (Biotrak II plate reader, Biochrom, Cambridge, UK). Cell viability (%) was calculated using the following equation: Cell viability (%) = [OD_{540} (sample)/OD_{540} (control)] × 100, where OD_{540} (sample) represents the optical density from the wells treated with siRNA/PEI complex, siRNA/Lipofectamine or siRNA/HHSC complex and OD_{540} (control) represents the optical density from the wells treated with PBS. The sensitivity of cells to siRNA/PEI complex, siRNA/Lipofectamine or siRNA/HHSCs complex was measured by IC_{50} (IC_{50} values defined as the concentration inducing 50% loss of cell viability).

2.2.5. Cellular uptake studies

2.2.5.1. Comparing uptake efficiencies of FITC labeled siRNA/HHSCs complex. SGC-7901 and GES-1 cells were plated in culture slides (Bedford, MA, USA) at a density of 2×10^5 cells/well in a 12 wells plate and incubated at 37 °C for 24 h, respectively. Then, the culture medium was replaced with 0.2 mL of serum free medium containing FITC-siRNA/HSCCs complex and FITC-siRNA/PEI (25k) complex with a weight ratio of 1:5. The culture slide was incubated at 37 °C and retrieved in 2 h. Complexes between Lipofectamine™ and siRNA were prepared as per the manufacture's protocol. Cells were fixed with 1 wt% paraformaldehyde and checked under the Fluorescence Inversion microscope for similar confluency and morphology (Nikon TE2000, JP) at an excitation wavelength of 488 nm. The magnification was 320. To determine the transfection efficiency, the cells were washed twice and lysised with Trypsin–EDTA solution and analyzed by FACS Calibur flow cytometer (BD, Biosciences, USA). Fluorescent signals were measured on a Mithras LB 940, corrected for background signals and expressed as relative to the signal of free siRNA. The relative geometrical mean fluorescence intensities (MFI) of cells incubated with FITC-siRNA/HHSCs, lipofetamine and PEI were compared with that treated with free siRNA using WinMDI 2.9 software. The percentage of cells that had internalized complexes was determined by the number of Green positive cells and expressed as transfection efficiency [% cells]. Generally, a minimum of 2×10^4 cells was analyzed in each measurement. The data were analyzed using Beckman Coulter CXP analysis software. All experiments were performed in triplicates.

2.2.5.2. Competitive inhibition study on cellular uptake of FITC labeled siRNA/HHSC-1 complex. To investigate whether siRNA/HHSC-1 complex was specifically taken up by SGC-7901 cells through HA receptor (CD_{44}) mediated endocytosis, an excess amount (10 mg/mL and 20 mg/mL) of HA (M_w: 9600) was added to the transfection medium to block the interaction between siRNA/HHSC-1 complex and HA receptor on the cell surface. siRNA/HHSC-1 complex transfected cells were post-transfected using 20 μg of siRNA/HHSC complex in the presence of 10 mg and 20 mg of HA. After 2 h, transfected cells were trypsinized and washed three times with PBS and fixed with 1% paraformaldehyde solution. The transfection efficiency of siRNA/HHSC-1 complex in the presence of free HA was monitored by flow cytometry as described above.

2.2.5.3. Exploring uptake pathways of HGC nanoparticles using endocytic inhibitors. To investigate the mechanism of internalization of HHSC and Lipofectamine, 2×10^5 SGC-7901 cells were seeded on a 35-mm glass-base dish (Iwaki, Chiba, Japan) in 2 mL of RPMI 1640 containing 10% FBS for 24 h. Before transfection, the cells were washed once with 1 mL of PBS and were pre-incubated with serum-free medium in the absence or presence of the following three compound for various times: phAsO (10 μg/mL) (inhibitor of clathrin-mediated endocytosis) at 37 °C for 30 min; amiloride (5 mM) (inhibitor of macropinocytosis) for 10 min; or filipin III (1 μg/mL) (inhibitor of caveolae-mediated endocytosis) for 1 h. Complexes were prepared at 5:1 HHSC: siRNA weight ratio then were added and incubated for 1 h at 37 °C in the presence or absence of inhibitors (Mudhakir et al., 2008). At the end of the incubation, the culture medium was removed, and the cells were washed once with ice-cold PBS supplemented with heparin (20 U/mL) (Khalil et al., 2004). The cells then were trypsinized and collected into an Eppendorf tube. The cells then were washed twice after pelleting by centrifugation (1500 rpm, 4 °C, 5 min) and were suspended in 1 mL of heparin–PBS. Finally, cells were suspended in 0.5 mL of PBS and filtered through a nylon mesh. The cells then were analyzed by a flow cytometer above.

2.2.6. Gene silencing study

2.2.6.1. TaqMan real-time reverse-transcription polymerase chain reaction (RT-PCR). Total RNA was isolated from monolayer culture of SGC-7901 pre-transfected with either 50 nM of siRNA/PEI 25k, siRNA/HHSC-1, siRNA/HHSC-2, siRNA/HHSC-3 complexes with weight ratio 1:5 or the negative control (naked siRNA) for 24 h using a Trizol solution. Briefly, 1 mL of Trizol solution was added to the constructs and homogenized thoroughly. 200 μL of chloroform was added to the homogenate with vortexing and then incubated at room temperature for 5 min. The homogenate was centrifuged at 4 °C for 15 min at 15,000 × *g*. An aqueous phase was separated with the addition of 500 μL of cold isopropanol and incubated for 10 min at room temperature. Samples were centrifuged at 4 °C for 10 min at 15,000 × *g* and RNA pellet was obtained. The RNA pellet was diluted with DEPC water to adjust the RNA concentration.

Down-regulation of COX-2 mRNA was determined by quantitative real-time RT-PCR, standardized by the corresponding β-actin internal control. Each amplification was performed for 35 cycles, one cycle profile consisted of denaturation at 94 °C for 30 s, annealing at 55 °C (COX-2 and β-actin) for 30 s and extension at 72 °C for 30 s. A sample without RNA was included in each RT-PCR as a negative control. Sequences of COX-2 and β-actin primers used are as follows: COX-2 upstream, 5′-TCAAGTCCCTGAGCATCTAC-3′; COX-2 downstream, 5′-CATTCCTACCAC CAGCAACC-3′; β-actin upstream, 5′-GAAACTACCTTCA ACTCCATC-3′; β-actin downstream, 5′-CGAGGCCAGGATGGA GCCGCC-3′. The size of the amplified products was 488 bp for COX-2 and 219 bp for β-actin, respectively. Quantitation of the amount of PCR product was performed after electrophoresis on 1.5% agarose gels and ethidium bromide staining. The pictures were digitized and analyzed with Scion image analysis software to determine the mean density of mRNA bands. The gene silencing efficiency (%) was calculated based on the relative intensity of mRNA band of control group in each well with respect to wells with mRNA band of transfection groups. The gene silencing efficiency (%) for each transfection group was tested at least in 3 independent experiments.

2.2.6.2. Western blot analysis of COX-2 protein. SGC-7901 cells were incubated in NP-40 lysis buffer containing 50 mM Tris (pH 7.4), 150 mM NaCl, 1 mM EGTA, 1% NP-40, 0.25% SDS, 1 mM sodium

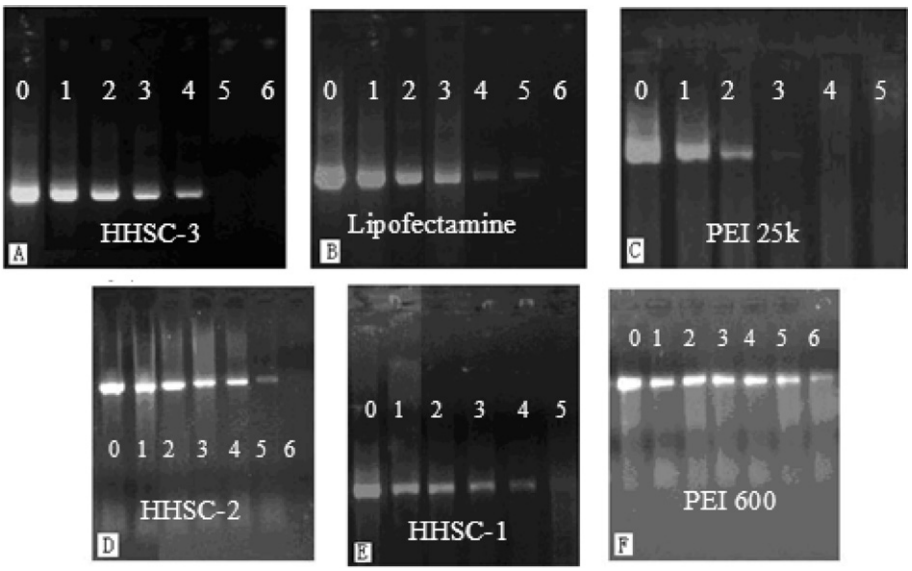

Fig. 1. Electrophoretic retardation analysis of siRNA binding by different carriers. The gel results for the individual HAPs are shown from (A) to (F). Lane numbers were corresponded to different HHSCs/siRNA weight ratios for (A) HHSC-3; (B) Lipofectamine 2000; (C) PEI 25k; (D) HHSC-2; (E) HHSC-1; (F) PEI 600; (1) 0 (siRNA only), (2) 0.5:1, (3) 1:1, (4) 2:1, (5) 5:1, (6) 10:1 and (7) 15:1. In the case of (c) and (e), the lane numbers correspond to: (1) 0 (siRNA only), (2) 0.5:1, (3) 1:1, (4) 2:1, (5) 5:1 and (6) 10:1.

vanadate, 1 mg/mL protease inhibitors, 200 μg/mL chymostatin and 1 mM PMSF for 30 min at 4 °C. Cell lysates were then centrifuged at 14,000 rpm for 10 min and supernatants were harvested. An aliquot of 10 mg of lysates was boiled and electrophoresed in 7.5% SDS-polyacrylamide gels under reducing conditions. The separated proteins were then electrophoretically transferred to a PVDF membrane (Immoblin-P, Millipore, Bedford, MA, USA). Following the reaction with a blocking solution of 10% non-fat dried milk for 1 h at room temperature, the membrane was probed with an anti-COX-2-specific antibody (Santa Cruz Biotech, Santa Cruz, CA, USA) or anti-β-actin antibody (Santa Cruz Biotech, Santa Cruz, CA, USA) at room temperature for 1 h. After washing with Tris-buffered saline containing 0.05% Tween-20 and incubation with horseradish peroxidase-conjugated secondary antibodies, protein bands were detected by the enhanced chemiluminescence method (Amersham Life Science, Piscataway, NJ, USA). Relative COX-2 protein concentrations were determined by densitometry of the scanned radiography image with the Quantity One 1-D Analysis v.4.5.2 software (Bio-Rad). All values were normalized for loading in comparison with the appropriate β-actin signal. The gene silencing efficiency (%) was calculated based on the relative intensity of protein band of control group in each well with respect to wells with protein band of transfection groups. The gene silencing efficiency (%) for each transfection group was tested at least in 3 independent experiments.

2.2.7. Statistical analysis

Statistical analysis was performed using a standard Student's *t*-test (comparing only two individual groups) with a minimum confidence level of 0.05 for significant statistical difference. All values are reported in term of mean and standard deviation.

3. Result and discussion

3.1. siRNA binding and formation of siRNA/HHSCs complexes

Agarose gel electrophoresis was utilized to detect complex formation between the synthesized HHSCs conjugates and the siRNA. This was based on the disappearance of free siRNA bands in agarose gels. As expected, the synthesized HHSCs were capable of effectively binding siRNA, resulting in retardation or disappearance of siRNA bands in agarose gel (Fig. 1(A, D, E)). When the weight ratios of carriers to siRNA were higher than 10:1, the migration of siRNA was completely retarded for all HHSCs (Fig. 2). The binding ability of the HHSCs was not significantly different from each other, but less than that of PEI 25k as indicated by a significant left shift in binding versus weight ratio plots (Fig. 1(C)). There were no obvious differences in siRNA binding capacity among the HHSCs, except that HHSC-3 showed a slightly higher siRNA binding ability in terms of weight ratio (inserted panel in Fig. 1(A)). The parent PEI 600 showed very low siRNA binding at all carriers:siRNA weight ratios tested, and PEI 25k showed complete siRNA binding even at very low carrier:siRNA weight ratio (about 1).

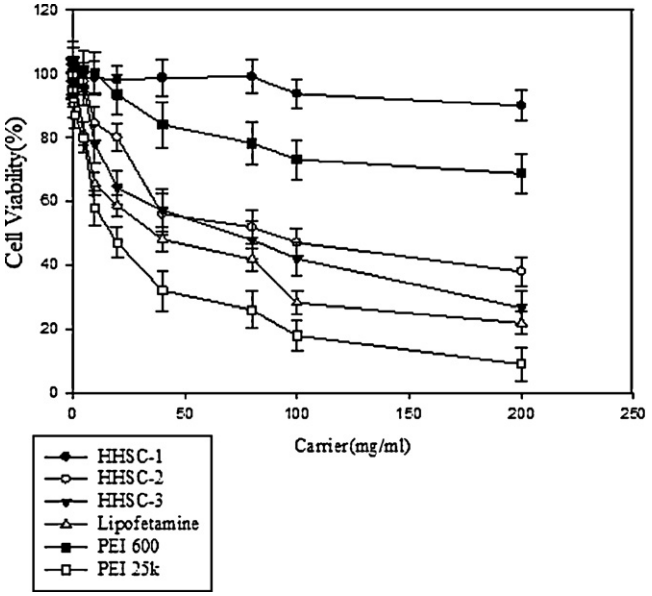

Fig. 2. Cytotoxicity of common siRNA condensing HHSCs, lipofetamine, and PEI complex with weight ratio from 1:1 to 1:200 ($n = 3$).

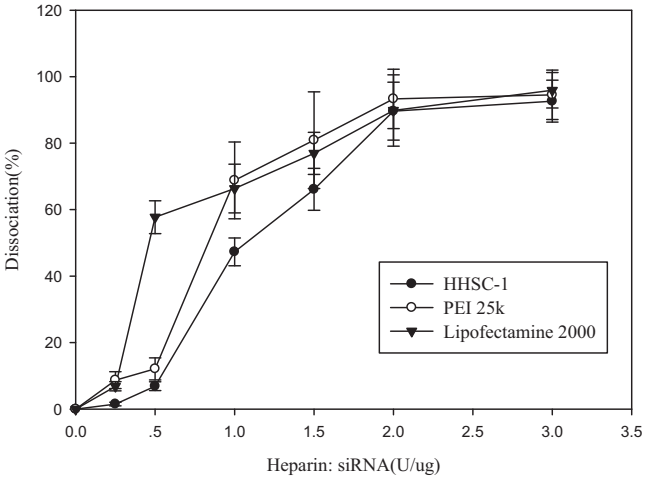

Fig. 3. siRNA dissociation from carriers by heparin competition and amount of complex at the ratio (w/w) of 1:5. The dissociation was determined assessing free siRNA by agarose gel electrophoresis. The data are the mean ± standard error for $n = 3$.

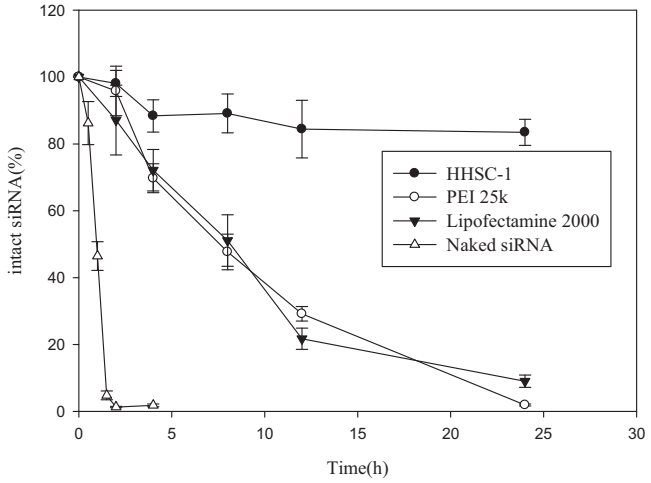

Fig. 4. The degradation kinetic profile of intact siRNA from HHSC-1 compared to Lipofectamine 2000 and PEI 25k in plasma in vitro at the ratio (w/w) of 1:5. The data show the weight percentage of intact siRNA recovered from carriers.

3.2. Cytotoxicity of siRNA/HHSCs complexes

The cytotoxicity of HHSCs was compared with that of PEI 25k, PEI 600, and Lipofectamine. It should be mentioned that HHSC-1/siRNA showed good cytocompatibility even at a high dose (HHSC-1:siRNA weight ratio up to 15:1). HHSC-1 provided higher cell viability than did HHSC-2 and HHSC-3. The use of HHSC-1 for delivery of siRNA (HHSC-1/siRNA weight ratio, 5/1) into SGC-7901 cells (Fig. 2) yielded 93.5 ± 2.0% viability at the concentration of 50 mg/mL. In contrast, complexes of siRNA with Lipofectamine and PEI 25k showed significant cytotoxicity particularly at high doses as shown in Fig. 2. HHSC-1 alone is also cytocompatible, exhibiting around 90% cell viability after 24 h incubation with concentration up to 200 mg/mL (Fig. 2) due to its lowest DS_p. The IC_{50} sequence of these carriers was HHSC-1 > PEI 600 > HHSC-2 > HHSC-3 > lipofetamine > PEI 25k. The low toxicity of the HHSC-1/siRNA complex suggests that repeated administration of a therapeutic gene may be feasible.

3.3. Release of siRNA from HHSCs/siRNA complex with polyanion heparin

siRNA complexes have to transfer the negatively charged cell membrane for RNAi. However, siRNA might take part in unwanted exchange with large polyanions found outside cells such as sulphated glycosaminoglycans during the transfer membrane due to its low charge density, and it reduces the siRNA delivery efficiency. Thus, it is important to measure the capability of complexes for siRNA delivery in vitro through the polyanion competition assay (Xiong et al., 2009). A competing polyanion, heparin sodium, was added at various concentrations to gradually induce the decomplexation of the condensed siRNA within the complexes.

The siRNA release from HHSC-1, PEI 25k and lipofetamine 2000 in the presence of heparin is summarized in Fig. 3. The siRNA release from its complex was dependent on heparin concentration. The ratio of heparin to polymer which leads to 50% of siRNA release (RR_{50}) from the complexes was used as a measure of propensity for dissociation (Xiong et al., 2009). Accordingly, HHSC-1 formed more stable complexes with siRNA as compared to PEI 25k and lipofetamine 2000, based on the higher RR_{50} values for the HHSC-1 complex (0.5 U/μg, heparin:carrier) as compared to the RR_{50} value of 0.75 and 1.0 U/μg (heparin:polymer) for PEI 25k and lipofetamine 2000, respectively. Complete siRNA release from all carriers was observed when heparin to polymer weight ratio reached 2.0:1.

3.4. Serum stability of siRNA from HHSCs/siRNA complex

The stability of siRNA in serum condition is also another important factor for siRNA delivery in vivo. The serum stability of siRNA/HHSC-1, PEI 25k and lipofetamine 2000 complexes were examined by exposing complexes to 25% FBS for 24 h prior to electrophoretic analysis. Uncomplexed siRNA was undetectable following exposure to serum for 2 h (Fig. 4). In contrast siRNA condensed with HHSC-1 prior to serum exposure was detectable in the well. For the HHSC-1/siRNA complex, even the lowest applied polymer:siRNA ratio (5:1) demonstrated a significant protective effect for siRNA where the percentages of intact siRNA in the complex reached 95% after 2 h. The synthesized HHSC-1 did demonstrate a significant difference in the siRNA protection ability. The presence of serum did not significantly affect the intracellular delivery efficiency of HHSC-1. Due to the shielding effect of HA, HHSCs are more stable in a serum-containing medium and may help to increase gene transfection efficiency.

3.5. Cellular uptake study

3.5.1. Transfection of siRNA by HHSC/siRNA complex

FITC labeled siRNA was used to visualize the receptor mediated endocytosis of siRNA/HHSCs complex. As mentioned earlier, cluster determinant 44 (CD_{44}), receptor for hyaluronate-mediated motility (RHAMM), and lymphatic vessel endothelial hyaluronan receptor-1 (LYVE-1) have been identified as HA receptors. SGC-7901 cells are reported to overexpress CD_{44} at which HA is taken up by the cells through the receptor-mediated endocytosis. Intracellular uptake of FITC-siRNA/HHSC-1 complex by SGC-7901 cells was compared with that of GES-1 cells without HA receptors. Widely used transfection agent, Lipofectamine™2000, was used for comparison with the cationic polymers synthesized in this study. In pre-experiment, we prepared siRNA/HHSCs complexes with different weight ratios (from 1:1 to 1:20) and the cellular uptake experiment was also carried out. From the Fluorescent images of the internalized FITC-siRNA from HHSCs complexes, the weight ratio of 1:5 (siRNA–HHSCs) could get the highest transfection efficiency. When the weight ratio >1:5, the HHSCs could not binding the total siRNA and when the weight ratio <1:5, the excess HHSCs may cause the cytotoxicity due to the positive charge. So in the cellular uptake and competitive inhibition experiments, the weight ratio of 1:5 (siRNA–HHSCs) was chosen to investigate the HA receptor (CD_{44}) mediated endocytosis.

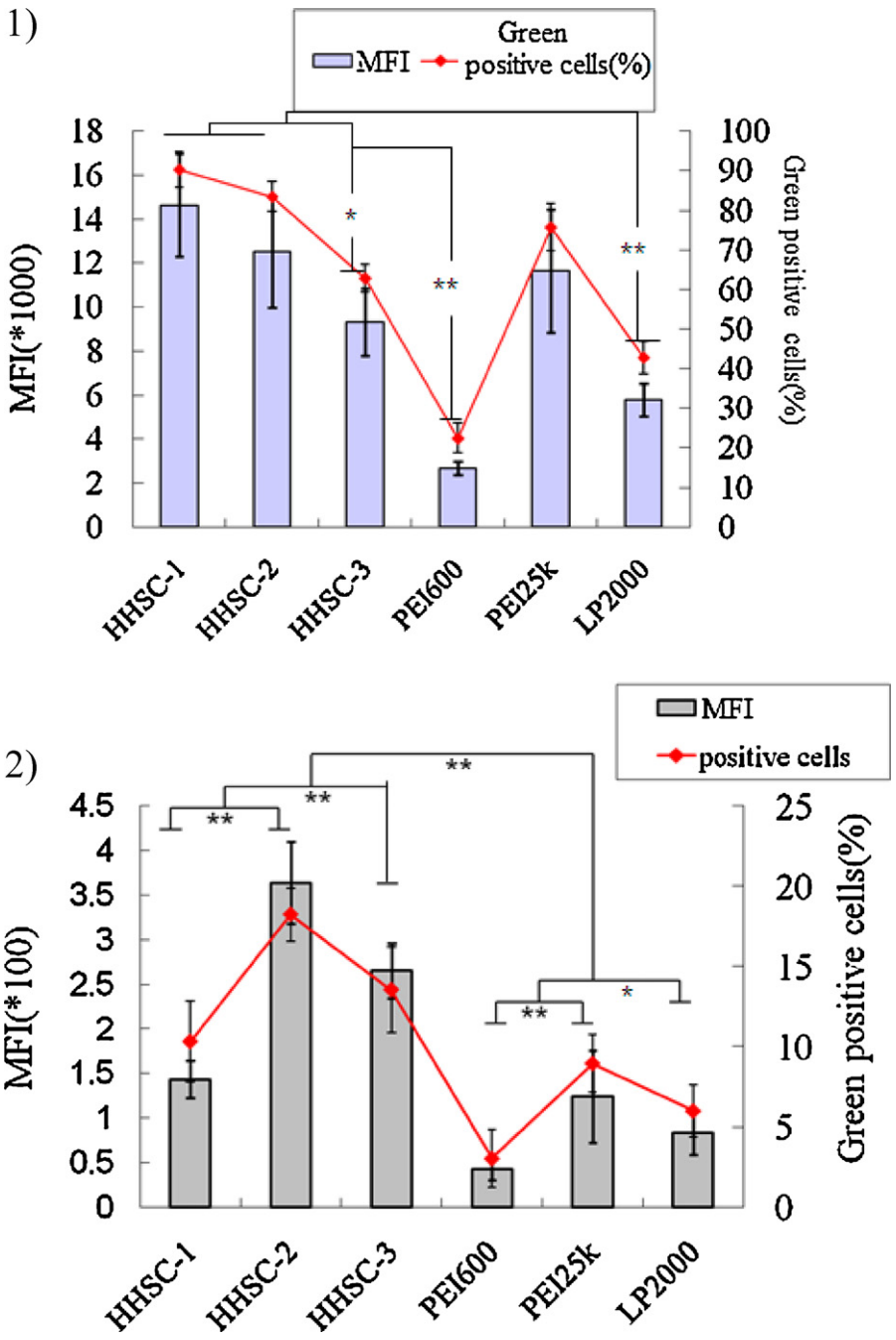

Fig. 5. (1) Uptake of fluorescent siRNA in SGC-7901 cells. Fluorescent siRNA was complexed to Lipofectamine2000, HHSCs, or PEI at carrier/siRNA weight ratio of 5:1. The mean fluorescence intensity (MFI) and relative gene transfection efficiency (positive cells, %) were analyzed by FACS. The results are expressed as the average of three independent experiments. *: Significantly different from other groups ($P<0.05$). **: Significantly different from other groups ($P<0.01$). (2) Uptake of fluorescent siRNA in GES-1 cells. Fluorescent siRNA was complexed to Lipofectamine2000, HHSCs, or PEI at carrier/siRNA weight ratio of 5:1. The mean fluorescence intensity (MFI) and relative gene transfection efficiency (positive cells, %) were analyzed by FACS. The results are expressed as the average of three independent experiments. *: Significantly different from other groups ($P<0.05$). **: Significantly different from other groups ($P<0.01$).

The delivery efficiency of HHSCs was comparable to that of Lipofectamine™2000, PEI 600 and PEI 25k. FACS analysis revealed that HHSCs increased the intracellular delivery of siRNA as compared with PEI and lipofetamine 2000. Fig. 5(1 and 2) displays the mean fluorescence intensity (MFI) of cells that have taken up complexes, and that is an indirect measure of the intracellular amount of siRNA. MFI of cells transfected with HHSCs was significantly higher than that of cells transfected with PEI and Lipofectamine™2000. The HHSC-1 was more stable with the higher cell uptake and low cytotoxicity, but the highest gene silencing efficiency was lower than the HHSC-2 complex does. Because the siRNA can make the gene silencing efficiency only to be released from the carriers and stay to be the free form in the cytoplasm. I think the binding efficiency of HHSC-1 was higher than HHSC-2, which make the siRNA more difficult to released from the HHSC-1 complex to be the free form than the HHSC2 complex. This conclusion may suggest that more stable, higher cell uptake and low cytotoxicity siRNA complexes did not have the higher gene silencing efficiency. The gene silencing efficiency is also depending on the siRNA which released from the carriers after uptaking by the cells. In Fig. 5(1 and 2), the large difference appears for the cellular uptake of siRNA/PEI125K complex between SGC-7901 cells and GES-1 cell. I think the toler-

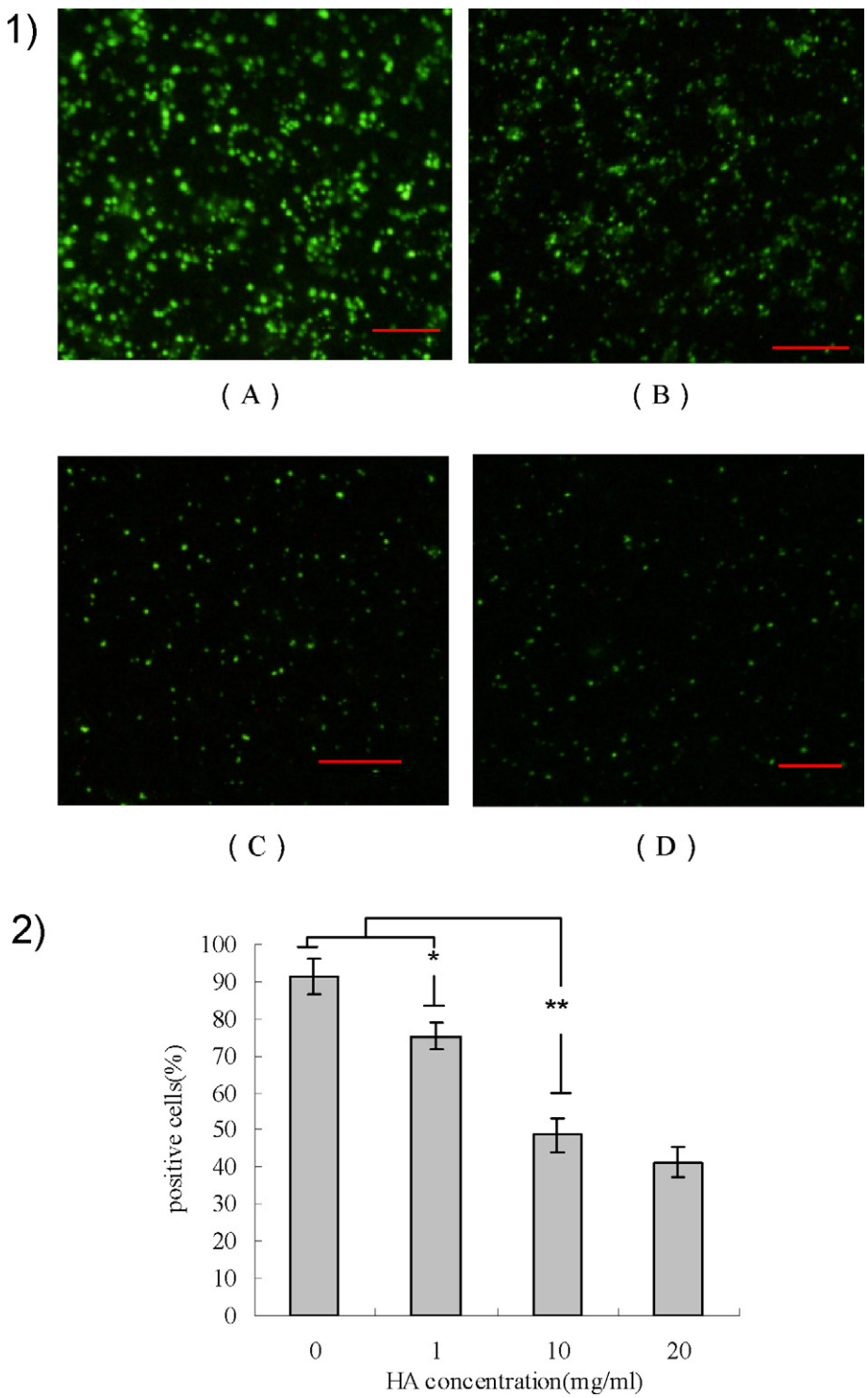

Fig. 6. (1) Fluorescent images of the internalized FAM-siRNA (green) from HHSC-1 complex (weight ratio of siRNA to HHSC-1 was 1:5) by SGC-7901 cell pretreated with different HA concentrations: A: control, B: 1 mg/mL, C: 10 mg/mL, D: 20 mg/mL with bars of 100 μm. (2) The cell uptake efficiency (%) of different FAM-siRNA from HHSC-1 complex (weight ratio of siRNA to HHSC-1 was 1:5) by SGC-7901 cell after treatment with different HA concentrations. The data are the mean ± standard error ($n = 3$). $^{**}P < 0.01$. (For interpretation of the references to color in this figure legend, the reader is referred to the web version of the article.)

ance of SGC-7901 was better than GES-1 when it was treated with siRNA/PEI125K complex. For GES-1 cells, siRNA/PEI125K complex may cause slight cytotoxicity which may have a negative effect for the cell uptake. But this conclusion will be checked by some experiments. Considering all these results, HA in the outer surface of siRNA/HHSCs complex was thought to significantly contribute to the improved cellular uptake by HA receptor mediated endocytosis making possible target specific delivery to the tissues with HA receptors.

3.5.2. *Inhibition of receptor mediated endocytosis (CD_{44}-HA interaction)*

Specific interaction of HA with CD_{44} receptors expressed on selected cancerous cells has been well described in literature (Jiang

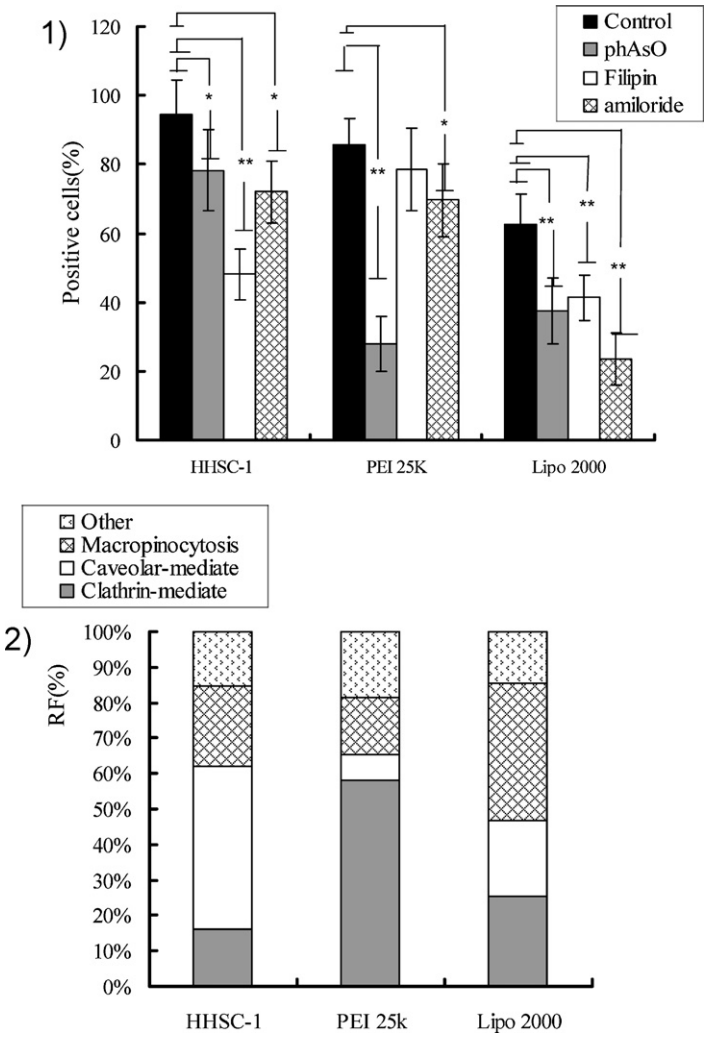

Fig. 7. (1) The uptake efficiency (%) of SGC-7901cells after treatment with different FITC-siRNA formulations (carrier/siRNA weight ratio of 5:1) with various cellular uptake inhibitors. The untreated cells were used as the reference group. The data are the mean ± standard error ($n = 3$). $^{*}P < 0.05$ vs control $^{**}P < 0.01$ vs control for each formulation. (2) The relative uptake ratio (RF, %) of each internalization pathway to the total internalization pathways of SGC-7901 cells after treatment with different FITC-siRNA formulations (carrier/siRNA weight ratio of 5:1).

et al., 2008, 2009; Surace et al., 2009). These studies suggested that HA could be used as a targeting moiety to some cancer cell lines. To prove that HHSCs were indeed transported within the cells via CD_{44} mediated endocytosis, the extent of the mean fluorescent intensity was quantitatively determined using a flow cytometry by adding an excess amount of low molecular weight soluble HA (M_w: 9600) in the transfection medium. Fig. 6(1) shows fluorescent intensity of SGC-7901 cells co-transfected with siRNA/HHSC complex, with and without soluble HA. The cellular fluorescence intensity of HHSC-1 pre-treated with free HA (10 mg/mL) was inferior to that of untreated one (Fig. 6(2), $P < 0.01$), while free HA (20 mg/mL) pre-treatment shows no significance with that of HA (10 mg/mL) pre-treatment. It was suggested that free HA could competitively bind to CD_{44} receptors against the siRNA/HHSC-1 complex resulting in the decreased fluorescent intensity. This indicates that the fluorescent intensity of HHSC-1 was reduced by competitive binding of free HA onto the CD_{44} receptors, thereby lowering the extent of cellular uptake via CD_{44} receptor mediated endocytosis.

3.5.2.1. Mechanisms of siRNA/HHSC-1 uptake. The effects of the macropinocytosis inhibitor, amiloride, the clathrin-mediated endocytosis inhibitor, phAsO, and the caveolar-mediated endocytosis inhibitor, filipin, on cellular uptake of HHSC-1, PEI and lipofetamine 2000 were quantified using FACS analysis. The uptake of HHSC-1 was inhibited by phAsO by 16% ($P < 0.05$), and amiloride and filipin inhibited HHSC-1 uptake by 22% ($P < 0.05$) and 47% ($P < 0.01$), respectively (Fig. 7(1)). In the case of PEI, phAsO and amiloride inhibited internalization by 58% ($P < 0.01$) and 17% ($P < 0.05$); however, filipin did not inhibit PEI uptake. In the case of lipofetamine 2000, phAsO, filipin and amiloride inhibited internalization by 25% ($P < 0.01$), 39% ($P < 0.01$) and 21% ($P < 0.01$), respectively; Taken together, the results of the cellular uptake mechanism studies suggest that the caveolae-mediated endocytosis is the major cellular uptake pathway for HHSC-1; whereas, macropinocytosis and clathrin-mediated endocytosis are the following routes of HHSC-1 internalization. From Fig. 7(2), all carriers have the fourth pathway for internalization, which is still not clear and need to be investigated (Conner and Schmid, 2003; Lechardeur and Lukacs, 2002). Caveolae-mediated endocytosis is not associated with a pH decrease, and is known to be a nondigestive route of external substances into the cellular compartment. Some nonenveloped viruses, such as simian virus 40, utilize this route for transfection to host cells and accumulate in a smooth endoplasmic reticulum compartment. Thus, HHSC internalized by caveolae-

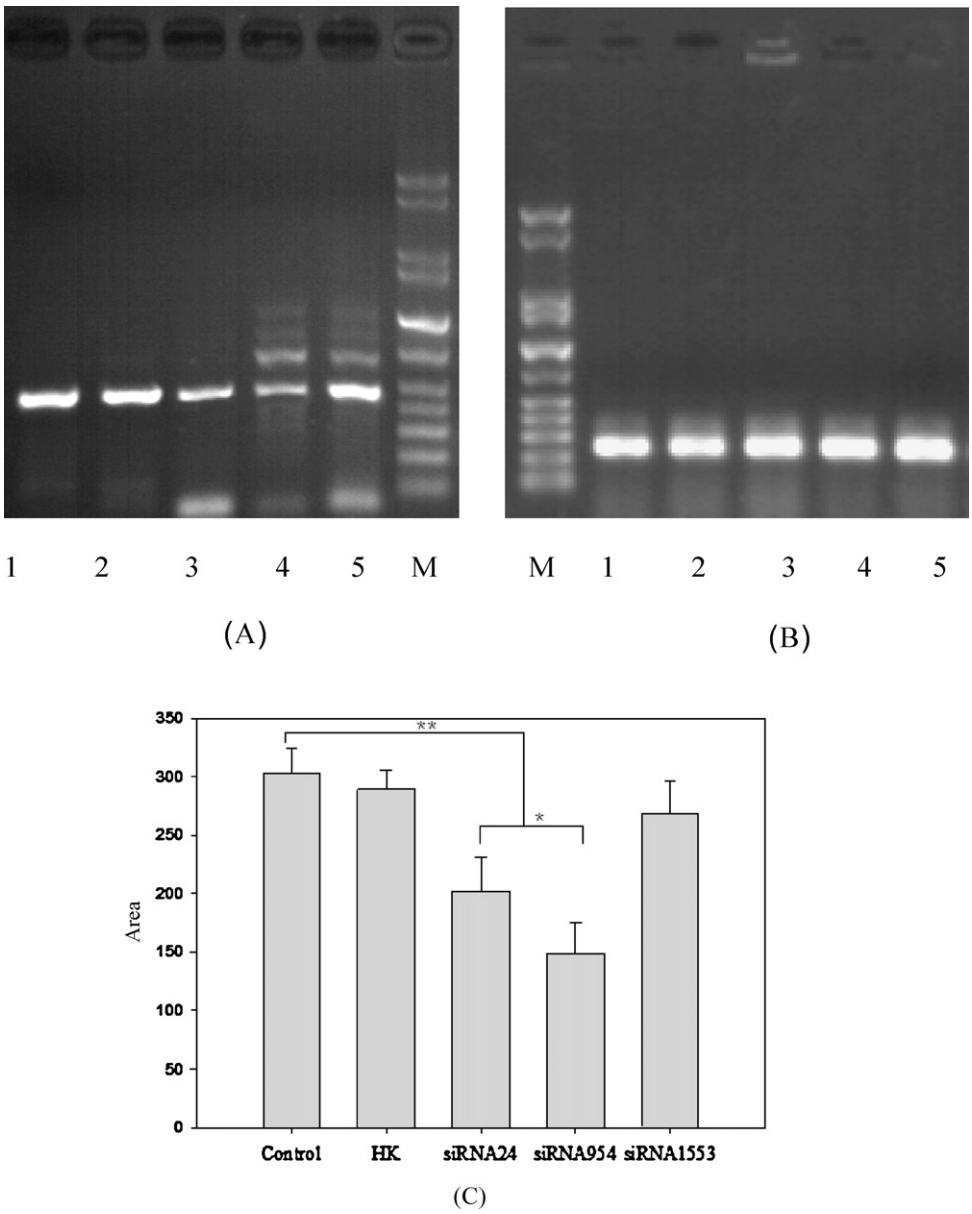

Fig. 8. Agarose gel electrophoresis of the gene silencing efficiency of siRNA interfering in the expression of COX-2 (A), β-actin (B) by RT-PCR method and (C) plots of the COX-2 mRNA content with different siRNA complexes (the weight ratio of siRNA to carriers was1:5, $^{*}P < 0.05$, $^{**}P < 0.01$). Lane M: 1 kb plus marker; lane 1: control; lane2: siRNA/PEI 25k; lane 3: siRNA/HHSC-1; lane 4: siRNA/HHSC-2; lane 5: siRNA/HHSC-3.

mediated endocytosis may be able to avoid siRNA degradation in acidic organelles, leading to high transfection efficiency (Nam et al., 2009; Oba et al., 2008).

It has been shown that the entry mechanism may depend on the size of the nanoparticles. Indeed, polysaccharide-based nanoparticles with a diameter less than 200 nm were exclusively internalized via clathrin-coated pits, whereas those of 500 nm entered the cells via caveolae (Rejman et al., 2004). The average diameter of our complexes, as determined by AFM, was around 200–500 nm. However, the size distribution of these complexes typically ranged between 300 and 450 nm, with more than 63% of the lipoplexes having a diameter larger than 200 nm. Therefore, from the size of the complexes a caveolae-mediated endocytosis pathway and to a lesser extend a clathrin-mediated caveolae-mediated pathway could be expected.

To improve the therapeutic potential of the nanoparticle-based carriers for the intracellular delivery, it is important to understand the physicochemical properties of nanoparticles affecting the cellular uptake mechanism and the intracellular trafficking. To date, several reports have discussed the internalization of nanoparticle-based carriers into the cells by endocytic pathways (Jensen et al., 2003; Meng et al., 2006; Panyam and Labhasetwar, 2003). Endocytosis is a conserved process in eukaryotes where extracellular substances are taken up into the cells usually by the invagination of plasma membrane forming vesicles. In addition to the classical clathrin- (or receptor-) mediated pathway, other endocytic mechanisms have been identified: phagocytosis, caveolae-mediated endocytosis, macropinocytosis, and clathrin- and caveolae-independent endocytosis (Conner and Schmid, 2003; Johannes and Lamaze, 2002; Khalil et al., 2006). These various endocytic routes vary in the composition of coat, size of the detached vesicles, and fate of the internalized material (Conner and Schmid, 2003; Khalil et al., 2006; Lamaze and Schmid, 1995). Each clathrin-mediated endocytosis pathway is initiated by a specific ligand–receptor interaction on the extracellular surface. Upon entry, internalized nanoparticles are generally entrapped in the

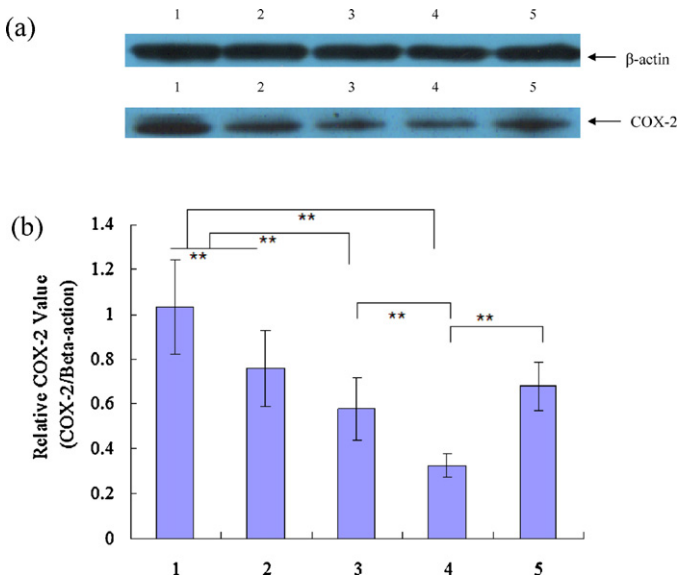

Fig. 9. (a) The gene silencing efficiency of siRNA interfering in the expression of COX-2 and β-actin by Western blot method. Lane 1: control; lane2: siRNA/PEI 25k; lane 3: siRNA/HHSC-1; lane 4: siRNA/HHSC-2; lane 5: siRNA/HHSC-3. The weight ratio of siRNA to carriers was 1:5. (b) Densitometry analysis of Western blots following COX-2 knockdown. 1: control; 2: siRNA/PEI 25k; 3: siRNA/HHSC-1; 4: siRNA/HHSC-2; 5: siRNA/HHSC-3. (**$P < 0.01$). The weight ratio of siRNA to carriers was 1:5.

intracellular vesicles (i.e., endosomes). Unfortunately, these endosomes tend to fuse with the acidic lysosomes later, and result in sequestration followed by degradation of the cargo therapeutics by the lysosomal enzymes (Watson et al., 2005). Accordingly, it is beneficial to develop strategies that can internalize nanoparticles preferentially through an alternative route. Pathways such as caveolar uptake and macropinocytosis are somewhat nonspecific, and neither acidic nor digestive (Conner and Schmid, 2003). Macropinocytosis involves large endocytic vesicles of irregular size and shape, which are formed from the actin-dependent lamellipodia (plasma membrane extensions). Therefore, this pathway may serve as a promising alternative to the clathrin-mediated endocytosis avoiding lysosomal degradation of the internalized nanoparticles.

3.6. The inhibitory effect on COX-2 expression

COX-2 over-expressing SGC-7901 cells were separately transfected with either 50 nM of siRNA/PEI 25k, siRNA/HHSC-1, siRNA/HHSC-2, siRNA/HHSC-3 complexes or the negative control (naked siRNA). The inhibitory effect on COX-2 expression was determined by Western blot analysis on the protein level and by TaqMan real-time RT-PCR on the mRNA level. As shown in Figs. 8 and 9(a and b), all three siRNA complexes down-regulated COX-2 gene expression. siRNA/HHSC-2 complex evoked the highest gene silencing efficiency, that is 73% at the protein ($P < 0.01$ compared with negative control) and 55.84% ($P < 0.01$ compared with negative control) at the mRNA level, whereas the control group did not.

4. Conclusion

A novel target specific intracellular gene delivery system was successfully developed using hydrophobized hyaluronic acid–spermine conjugates (HHSCs). HHSCs appeared less cytotoxic than PEI and lipofetamine 2000 because of the negatively charged HA which reduced the positive charge density of the complexes. We demonstrated that all HHSCs can effectively bind siRNA and protect siRNA from degradation by nuclease in serum. FITC-siRNA/HHSC complex could be taken up well by SGC-7901 cells through the CD_{44}-HA receptor mediated endocytosis. In addition, the siRNA uptake efficiency of siRNA/HHSC-1 complex was more efficient in the CD_{44} over-expressing SGC-7901cells than in GES-1 cells without HA receptors. The transfection efficiency was reduced in the presence of free HA in the transfection medium, reflecting that siRNA/HHSC-1 complex was selectively taken up by SGC-7901 cells via the receptor mediated endocytosis. The mechanisms of cellular uptake of HHSC-1 were examined regarding different endocytic pathways. Results indicated that siRNA/HHSC-1 complex was preferentially internalized by caveolae-mediated endocytosis via nonacidic and nondegradable intracellular compartments. The novel conjugate, which can deliver siRNA specifically to the cells containing HA receptor, will be investigated further for in vivo applications.

Acknowledgments

The authors thank partial financial support from Ministry of Science and Technology of the People's Republic of China under project 2009ZX09310-004 and the National Natural Science Foundation of China Project (Grant no. 81072588).

References

Azzam, T., Eliyahu, H., Makovitzki, A., Linial, M., Domb, A.J., 2004. Hydrophobized dextran–spermine conjugate as potential vector for in vitro gene transfection. J. Control Release 96, 309–323.
Bolcato-Bellemin, A.L., Bonnet, M.E., Creusat, G., Erbacher, P., Behr, J.P., 2007. Sticky overhangs enhance siRNA-mediated gene silencing. Proc. Natl. Acad. Sci. U.S.A. 104, 16050–16055.
Breunig, M., Hozsa, C., Lungwitz, U., Watanabe, K., Umeda, I., Kato, H., Goepferich, A., 2008. Mechanistic investigation of poly(ethylene imine)-based siRNA delivery: disulfide bonds boost intracellular release of the cargo. J. Control Release 130, 57–63.
Cavallaro, G., Scire, S., Licciardi, M., Ogris, M., Wagner, E., Giammona, G., 2008. Polyhydroxyethylaspartamide–spermine copolymers: efficient vectors for gene delivery. J. Control Release 131, 54–63.
Conner, S.D., Schmid, S.L., 2003. Regulated portals of entry into the cell. Nature 422, 37–44.
Coradini, D., Pellizzaro, C., Miglierini, G., Daidone, M.G., Perbellini, A., 1999. Hyaluronic acid as drug delivery for sodium butyrate: improvement of the anti-proliferative activity on a breast-cancer cell line. Int. J. Cancer 81, 411–416.
Eliaz, R.E., Szoka Jr., F.C., 2001. Liposome-encapsulated doxorubicin targeted to CD44: a strategy to kill CD44-overexpressing tumor cells. Cancer Res. 61, 2592–2601.
Eliyahu, H., Joseph, A., Azzam, T., Barenholz, Y., Domb, A.J., 2006a. Dextran–spermine-based polyplexes – evaluation of transgene expression and of local and systemic toxicity in mice. Biomaterials 27, 1636–1645.
Eliyahu, H., Siani, S., Azzam, T., Domb, A.J., Barenholz, Y., 2006b. Relationships between chemical composition, physical properties and transfection efficiency of polysaccharide–spermine conjugates. Biomaterials 27, 1646–1655.
Eliyahu, H., Joseph, A., Schillemans, J.P., Azzam, T., Domb, A.J., Barenholz, Y., 2007. Characterization and in vivo performance of dextran–spermine polyplexes and DOTAP/cholesterol lipoplexes administered locally and systemically. Biomaterials 28, 2339–2349.
Elron-Gross, I., Glucksam, Y., Melikhov, D., Margalit, R., 2008. Cyclooxygenase inhibition by diclofenac formulated in bioadhesive carriers. Biochim. Biophys. Acta 1778, 931–936.
Hannon, G.J., 2002. RNA interference. Nature 418, 244–251.
Jensen, K.D., Nori, A., Tijerina, M., Kopeckova, P., Kopecek, J., 2003. Cytoplasmic delivery and nuclear targeting of synthetic macromolecules. J. Control Release 87, 89–105.
Jeon, O., Yang, H.S., Lee, T.J., Kim, B.S., 2008. Heparin-conjugated polyethylenimine for gene delivery. J. Control Release 132, 236–242.
Jere, D., Jiang, H.L., Kim, Y.K., Arote, R., Choi, Y.J., Yun, C.H., Cho, M.H., Cho, C.S., 2009. Chitosan-graft-polyethylenimine for Akt1 siRNA delivery to lung cancer cells. Int. J. Pharm. 378, 194–200.
Jiang, G., Park, K., Kim, J., Kim, K.S., Hahn, S.K., 2009. Target specific intracellular delivery of siRNA/PEI-HA complex by receptor mediated endocytosis. Mol. Pharmacol. 6, 727–737.
Jiang, G., Park, K., Kim, J., Kim, K.S., Oh, E.J., Kang, H., Han, S.E., Oh, Y.K., Park, T.G., Kwang Hahn, S., 2008. Hyaluronic acid–polyethyleneimine conjugate for target specific intracellular delivery of siRNA. Biopolymers 89, 635–642.
Johannes, L., Lamaze, C., 2002. Clathrin-dependent or not: is it still the question? Traffic 3, 443–451.

Ke, Y., Ning, T., Wang, B., 1994. Establishment and characterization of a SV40 transformed human fetal gastric epithelial cell line-GES-1. Zhonghua Zhong Liu Za Zhi 16, 7–10.
Khalil, I.A., Futaki, S., Niwa, M., Baba, Y., Kaji, N., Kamiya, H., Harashima, H., 2004. Mechanism of improved gene transfer by the N-terminal stearylation of octaarginine: enhanced cellular association by hydrophobic core formation. Gene Ther. 11, 636–644.
Khalil, I.A., Kogure, K., Akita, H., Harashima, H., 2006. Uptake pathways and subsequent intracellular trafficking in nonviral gene delivery. Pharmacol. Rev. 58, 32–45.
Kim, S.H., Jeong, J.H., Lee, S.H., Kim, S.W., Park, T.G., 2006. PEG conjugated VEGF siRNA for anti-angiogenic gene therapy. J. Control Release 116, 123–129.
Kleinman, M.E., Yamada, K., Takeda, A., Chandrasekaran, V., Nozaki, M., Baffi, J.Z., Albuquerque, R.J., Yamasaki, S., Itaya, M., Pan, Y., Appukuttan, B., Gibbs, D., Yang, Z., Kariko, K., Ambati, B.K., Wilgus, T.A., DiPietro, L.A., Sakurai, E., Zhang, K., Smith, J.R., Taylor, E.W., Ambati, J., 2008. Sequence- and target-independent angiogenesis suppression by siRNA via TLR3. Nature 452, 591–597.
Lamaze, C., Schmid, S.L., 1995. The emergence of clathrin-independent pinocytic pathways. Curr. Opin. Cell Biol. 7, 573–580.
Lechardeur, D., Lukacs, G.L., 2002. Intracellular barriers to non-viral gene transfer. Curr. Gene Ther. 2, 183–194.
Lee, H., Mok, H., Lee, S., Oh, Y.K., Park, T.G., 2007. Target-specific intracellular delivery of siRNA using degradable hyaluronic acid nanogels. J. Control Release 119, 245–252.
Luo, Y., Ziebell, M.R., Prestwich, G.D., 2000. A hyaluronic acid–taxol antitumor bioconjugate targeted to cancer cells. Biomacromolecules 1, 208–218.
Meng, W., Parker, T.L., Kallinteri, P., Walker, D.A., Higgins, S., Hutcheon, G.A., Garnett, M.C., 2006. Uptake and metabolism of novel biodegradable poly (glycerol-adipate) nanoparticles in DAOY monolayer. J. Control Release 116, 314–321.
Mok, H., Park, T.G., 2008. Self-crosslinked and reducible fusogenic peptides for intracellular delivery of siRNA. Biopolymers 89, 881–888.
Mudhakir, D., Akita, H., Tan, E., Harashima, H., 2008. A novel IRQ ligand-modified nano-carrier targeted to a unique pathway of caveolar endocytic pathway. J. Control Release 125, 164–173.
Nam, H.Y., Kwon, S.M., Chung, H., Lee, S.Y., Kwon, S.H., Jeon, H., Kim, Y., Park, J.H., Kim, J., Her, S., Oh, Y.K., Kwon, I.C., Kim, K., Jeong, S.Y., 2009. Cellular uptake mechanism and intracellular fate of hydrophobically modified glycol chitosan nanoparticles. J. Control Release 135, 259–267.
Oba, M., Aoyagi, K., Miyata, K., Matsumoto, Y., Itaka, K., Nishiyama, N., Yamasaki, Y., Koyama, H., Kataoka, K., 2008. Polyplex micelles with cyclic RGD peptide ligands and disulfide cross-links directing to the enhanced transfection via controlled intracellular trafficking. Mol. Pharmacol. 5, 1080–1092.
Oishi, M., Nagasaki, Y., Itaka, K., Nishiyama, N., Kataoka, K., 2005. Lactosylated poly(ethylene glycol)-siRNA conjugate through acid-labile beta-thiopropionate linkage to construct pH-sensitive polyion complex micelles achieving enhanced gene silencing in hepatoma cells. J. Am. Chem. Soc. 127, 1624–1625.
Panyam, J., Labhasetwar, V., 2003. Dynamics of endocytosis and exocytosis of poly(D,L-lactide-co-glycolide) nanoparticles in vascular smooth muscle cells. Pharm. Res. 20, 212–220.
Prakash, T.P., Allerson, C.R., Dande, P., Vickers, T.A., Sioufi, N., Jarres, R., Baker, B.F., Swayze, E.E., Griffey, R.H., Bhat, B., 2005. Positional effect of chemical modifications on short interference RNA activity in mammalian cells. J. Med. Chem. 48, 4247–4253.
Rejman, J., Oberle, V., Zuhorn, I.S., Hoekstra, D., 2004. Size-dependent internalization of particles via the pathways of clathrin- and caveolae-mediated endocytosis. Biochem. J. 377, 159–169.
Schiffelers, R.M., Ansari, A., Xu, J., Zhou, Q., Tang, Q., Storm, G., Molema, G., Lu, P.Y., Scaria, P.V., Woodle, M.C., 2004. Cancer siRNA therapy by tumor selective delivery with ligand-targeted sterically stabilized nanoparticle. Nucleic Acids Res. 32, e149.
Shen, Y., Li, Q., Tu, J., Zhu, J., 2009. Synthesis and characterization of low molecular weight hyaluronic acid-based cationic micelles for efficient siRNA delivery. Carbohydr. Polym. 77, 95–104.
Soutschek, J., Akinc, A., Bramlage, B., Charisse, K., Constien, R., Donoghue, M., Elbashir, S., Geick, A., Hadwiger, P., Harborth, J., John, M., Kesavan, V., Lavine, G., Pandey, R.K., Racie, T., Rajeev, K.G., Rohl, I., Toudjarska, I., Wang, G., Wuschko, S., Bumcrot, D., Koteliansky, V., Limmer, S., Manoharan, M., Vornlocher, H.P., 2004. Therapeutic silencing of an endogenous gene by systemic administration of modified siRNAs. Nature 432, 173–178.
Surace, C., Arpicco, S., Dufay-Wojcicki, A., Marsaud, V., Bouclier, C., Clay, D., Cattel, L., Renoir, J.M., Fattal, E., 2009. Lipoplexes targeting the CD44 hyaluronic acid receptor for efficient transfection of breast cancer cells. Mol. Pharmacol. 6, 1062–1073.
Turley, E.A., 1989. The Biology of Hyaluronan. J. Wiley & Sons, Ltd., Chichester, UK.
Wang, X.L., Xu, R., Lu, Z.R., 2009. A peptide-targeted delivery system with pH-sensitive amphiphilic cell membrane disruption for efficient receptor-mediated siRNA delivery. J. Control Release 134, 207–213.
Watson, P., Jones, A.T., Stephens, D.J., 2005. Intracellular trafficking pathways and drug delivery: fluorescence imaging of living and fixed cells. Adv. Drug Deliv. Rev. 57, 43–61.
Wilson, A., Zhou, W., Champion, H.C., Alber, S., Tang, Z.L., Kennel, S., Watkins, S., Huang, L., Pitt, B., Li, S., 2005. Targeted delivery of oligodeoxynucleotides to mouse lung endothelial cells in vitro and in vivo. Mol. Ther. 12, 510–518.
Xiong, X.B., Uludag, H., Lavasanifar, A., 2009. Biodegradable amphiphilic poly(ethylene oxide)-block-polyesters with grafted polyamines as supramolecular nanocarriers for efficient siRNA delivery. Biomaterials 30, 242–253.
Yerushalmi, N., Arad, A., Margalit, R., 1994. Molecular and cellular studies of hyaluronic acid-modified liposomes as bioadhesive carriers for topical drug delivery in wound healing. Arch. Biochem. Biophys. 313, 267–273.
Yerushalmi, N., Margalit, R., 1998. Hyaluronic acid-modified bioadhesive liposomes as local drug depots: effects of cellular and fluid dynamics on liposome retention at target sites. Arch. Biochem. Biophys. 349, 21–26.